ADVANCES IN ATMOSPHERIC SCIENCES, VOL. 29, NO. 4, 2012, 755–768

Contrasts of Atmospheric Circulation and Associated Tropical Convection between Huaihe River Valley and Yangtze River Valley Mei-yu Flooding

HONG Jieli[1,2] (洪洁莉) and LIU Yimin*[1] (刘屹岷)

[1] *State Key Laboratory of Numerical Modeling for Atmospheric Sciences and Geophysical Fluid Dynamics, Institute of Atmospheric Physics, Chinese Academy of Sciences, Beijing* 100029

[2] *Graduate University of Chinese Academy of Sciences, Beijing* 100049

(Received 1 November 2011; revised 2 January 2012)

ABSTRACT

The significant differences of atmospheric circulation between flooding in the Huaihe and Yangtze River valleys during early mei-yu (i.e., the East Asian rainy season in June) and the related tropical convection were investigated. During the both flooding cases, although the geopotential height anomalies always exhibit equivalent barotropic structures in middle to high latitudes at middle and upper troposphere, the phase of the Rossby wave train is different over Eurasian continent. During flooding in the Huaihe River valley, only one single blocking anticyclone is located over Baikal Lake. In contrast, during flooding in the Yangtze River valley, there are two blocking anticyclones. One is over the Ural Mountains and the other is over Northeast Asia. In the lower troposphere a positive geopotential height anomaly is located at the western ridge of subtropical anticyclone over Western Pacific (SAWP) in both flooding cases, but the location of the height anomaly is much farther north and west during the Huaihe River mei-yu flooding. Furthermore, abnormal rainfall in the Huaihe River valley and the regions north of it in China is closely linked with the latent heating anomaly over the Arabian Sea and Indian peninsula. However, the rainfall in the Yangtze River valley and the regions to its south in China is strongly related to the convection over the western tropical Pacific. Numerical experiments demonstrated that the enhanced latent heating over the Arabian Sea and Indian peninsula causes water vapor convergence in the region south of Tibetan Plateau and in the Huaihe River valley extending to Japan Sea with enhanced precipitation; and vapor divergence over the Yangtze River valley and the regions to its south with deficient precipitation. While the weakened convection in the tropical West Pacific results in moisture converging over the Yangtze River and the region to its south, along with abundant rainfall.

Key words: Huaihe River, Yangtze River, mei-yu flooding, tropical convection heating anomaly

Citation: Hong, J. L., and Y. M. Liu, 2012: Contrasts of atmospheric circulation and associated tropical convection between Huaihe River valley and Yangtze River valley mei-yu flooding. *Adv. Atmos. Sci.*, **29**(4), 755–768, doi: 10.1007/s00376-012-1217-6.

1. Introduction

China is located in East Asia, which is influenced strongly by the summer monsoon system. The early summer climate of East Asia is characterized by a quasi-stationary rainband that extends from southeastern China to Japan in June and July (Tao and Chen, 1987). This rain band is known as the mei-yu front in China. Excessive precipitation related to mei-yu causes flooding that is economically costly and threatens human life. Many researchers have focused on finding the causes of the flooding and have attempted to forecast the location and duration of the flooding. Previous studies investigated the causes of flooding in Yangtze-Huaihe River valley during summer and the associated sustained, large-scale, abnormal atmospheric circulation with flooding. Tao and Chen (1987) systematically proposed that the East

*Corresponding author: LIU Yimin, lym@lasg.iap.ac.cn

© China National Committee for International Association of Meteorology and Atmospheric Sciences (IAMAS), Institute of Atmospheric Physics (IAP) and Science Press and Springer-Verlag Berlin Heidelberg 2012

Asian summer monsoon system is composed of a monsoon trough in South China Sea, the mei-yu front, the subtropical anticyclone over the Western Pacific (SAWP), the Tibetan High and cold air from the north. Tao and Wei (2006) emphasized the influence of Rossby waves on the summer climate of East Asia. However, these components interact with each other, making the forecasting of flooding very difficult. Zhang and Tao (1998) suggested that precipitation affecting the Yangtze-Huaihe Rivers valley is not only affected by southwesterly trade winds from the Bay of Bengal (BOB) and the Indo-China Peninsula but also by the SAWP and cold air from middle and high latitudes. Xu et al. (2001) demonstrated that during the early mei-yu period the SAWP jumps northward in the central Pacific and then expands westward. This phenomenon may be influenced by anomalous convection in the Intertropical Convergence Zone (ITCZ) and the northern BOB. Wu et al. (2008) presented the three-dimensional structure of subtropical anticyclone that favors the occurrence of persistent heavy rainfall over the Yangtze and Huaihe River valleys. Guo and Liu (2008) and Yao et al. (2007) demonstrated that the propagation of vorticity perturbations eastward in low latitudes and westward at middle latitudes causes baroclinic instability and results in the variation of the SAWP and the occurrence of heavy summer rainfall over East China. These studies showed that mei-yu flooding is affected not only by the circulation in subtropics but also by tropical and mid-latitude circulation systems.

The mei-yu rainband displays large variability on time scales ranging from hours to interannual even to interdecadal, and its geographical location varies from South China, Yangtze River to the Huaihe River. In most of the aforementioned studies, "Yangtze River-Huaihe River valleys", as a whole, are broadly used to describe the location of the mei-yu flooding. Flooding mostly occurs over the two valleys, but the differences between them have not been rigorously investigated. One obvious reason is that the distance between the two valleys is $< 5°$ latitude. However, in recent years such as 2003 and 2007, flooding in the Huaihe River valley has drawn meteorologists' attention. Flooding during these years is different from that in 1998 and 1999, when severe flooding mostly took place over the Yangtze River valley. So in recent years, many studies (e.g., Wang and Wang, 2002; Zhao et al., 2005, Wei and Zhang, 2009; Ma et al., 2011; Xuan et al., 2011) have focused on Huaihe River valley flooding. These studies have presented the circulation characteristics in individual Huaihe River flooding years and have revealed the connection between mei-yu flooding and the Pacific SSTA and the East Asian Westerly Jet.

The mei-yu front commences in June and ends in July. However, atmospheric circulation differs between June and July. As we know, the first impetus of monsoon is solar radiation. As solar radiation advances northward from June to July, the summer monsoon system responds. Therefore, under different mean states the key factors influencing atmospheric circulation anomalies are altered accordingly. Wang et al. (2009) showed that the East Asia summer monsoon could be divided into early summer [May–June (MJ)] and late summer [July–August (JA)] and the differences in mean state between MJ and JA are remarkable. In this study, we considered it necessary to differentiate atmospheric responses to different climate mean states that influence precipitation anomalies during mei-yu. Although many high-quality studies have focused on typical individual flooding cases during the mei-yu front, few studies have investigated the universal flooding characteristics related to it. To investigate the mechanism for large-scale and persistent heavy rainfall, we used long-term data from 1979–2007 to calculate universal differences in atmospheric circulation between flooding in the Huaihe and Yangtze River valleys during the early mei-yu.

The mei-yu embodies the East Asian summer monsoon, which is influenced by external forces and internal dynamic adjustments (Lau et al., 2000). Large-scale heat sources and sinks have dynamical influences on the quasi-stationary mean motion of the atmosphere (Smagorinsky, 1953). Many studies have revealed the relationship of East Asian summer monsoon with regard to the thermal status of the ocean, land, snow, and ice. Huang et al. (2003) reviewed the factors that can affect variability of the East Asian Monsoon: as ENSO events in the Pacific, Indian Ocean warming, sensible heating in arid and semiarid regions of northwest China, and thermal conditions of the TP. Other researchers have focused on the internal dynamics of monsoon. The dramatic nature of monsoon activity suggests that a positive feedback exists between heating and low-level circulation (Rodwell and Hoskins, 2001; Hagos and Zhang, 2010). Hoskins and Rodwell (1995) used an idealized model to confirm that diabatic heating is important to the formation of mean-state flow during summer. Studies by Wu et al. (1999, 2008), Wu and Liu (2000, 2003), and Liu et al. (1999, 2001a, 2004) showed that the effect of spatially nonuniform heating is the key for the formation and variation of subtropical highs based on their analyses of observational data and numerical simulation results. All of these studies provide theoretical support and idea for our investigation of the role of diabatic heating anomalies with regard to different atmospheric circulations, leading to flooding in the Huaihe and Yangtze River valleys during early mei-yu.

In the following section, the datasets and the atmospheric general circulation model (AGCM) used in this paper are described. Section 3 presents analysis of observational data to determine the differences in atmospheric circulation between flooding in the Huaihe and Yangtze River valleys during June, and the effect of latent heating of the key areas on atmospheric circulation during flooding is proposed. Section 4 demonstrates the atmospheric circulation and rainfall responses to latent heating anomalies in key regions affecting location of rainband in June using numerical experiments to further clarify the mechanism of latent heating. Section 5 provides a discussion of the implications of our results and a summary.

2. Methods

2.1 *Data*

The daily precipitation dataset of 743 stations in China for the period 1951–2007 was acquired from the National Meteorological Center of the China Meteorological Administration. The global monthly observational dataset for larger-scale precipitation distribution merging satellite-gauge product was provided by the Global Precipitation Climatology Project (GPCP) in this study. The Japanese 25-year Reanalysis (JRA-25) is an atmospheric reanalysis product that uses a recently developed numerical assimilation and forecast system of the Japan Meteorological Agency. We used its monthly data (horizontal resolution 1.125°) covering 29 years from 1979 to 2007. The dataset contains variables such as wind, geopotential height, longwave radiation, shortwave radiation, sensible heating flux, total column latent heating, and so on. In recent years, numerous investigators have studied the decadal and interdecadal variability of precipitation in China as well as in East Asia. They found decadal variation of the summer precipitation in East China occurring in the late 1970s (Huang et al., 1999; Chang et al., 2000; Zhou and Huang, 2003; Ding et al., 2007). Due to the lack of a long-term diabatic heating dataset, all of the datasets used in our analysis were from 1979 to 2007.

To extract the difference between Huaihe and Yangtze Rivers flooding, composite analyses were applied. In addition to this method, the singular value decomposition (SVD) analysis (Bretherton et al., 1992) was also used to identify important coupled modes between geopotential height anomaly at 200 hPa and precipitation in China during June.

To define the domain of the Huaihe River valley and the Yangtze River valley, respectively, we followed the method of Ting and Wang (1997). We calculated the correlation between precipitation at the central station of each river valley and at the remaining stations in China during June. The relevant areas with correlation coefficient surpassing the 95% confidence level were defined as the domain of flooding in the two valleys in June. Therefore, the stations in the flooding domains were considered to have similar precipitation patterns. In our study, the Huaihe River valley center was located in Suxian (33.38°N, 116.59°E), and the Yangtze River valley center was located in Tunxi (29.43°N, 118.17°E) (Figs. 1a and b). The center stations were selected based on their geographical position in the center of valley and their long-term records.

We used precipitation averaged over the two do-

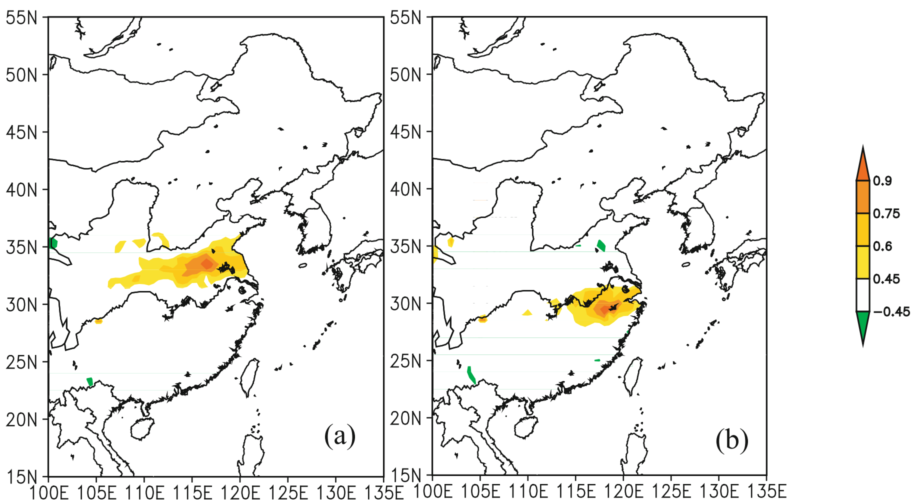

Fig. 1. Correlation of rainfall in each valley center station with rainfall in all stations of China. (a) Suxian centers in Huaihe River valley; (b) Tunxi centers in the Yangtze River valley.

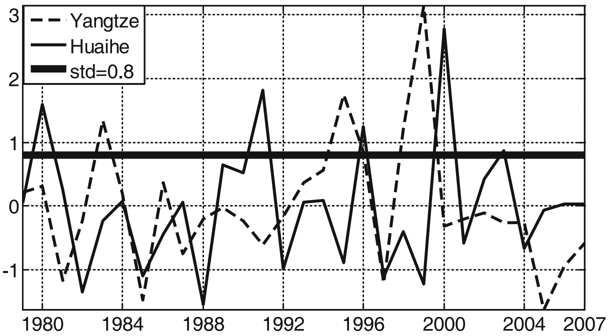

Fig. 2. Normalized June precipitation time series of Huaihe River valley and Yangtze River valley. The horizontal bold line denotes 0.8 standard deviation.

mains as the precipitation indices for the two valleys in June, to determine the two indices after they were normalized with their standard deviations (SD) (Fig. 2). Years in which SD was >0.8 SD were defined as flooding years, following the criterion of Ding and Wang (2005). Notably, in 1996 flooding occurred in both the Huaihe and Yangtze River valleys. To identify the contrast between them more clearly, 1996 was eliminated from flooding years for composite analysis. Accordingly, mei-yu flooding in the Huaihe River valley took place in 1980, 1991, 2000, and 2003, and in the Yangtze River valley in 1983, 1995, 1998, and 1999. Flooding in 2005 and 2007 was excluded because it occurred mostly in July and not in June.

2.2 *AGCM*

The AGCM used in this study is the Spectral Atmospheric Model (SAMIL) (Wu et al., 1996; Wu et al., 2004; Wang et al., 2004; Bao et al., 2006), developed by the State Key Laboratory of Numerical Modeling for Atmospheric Sciences and Geophysical Fluid Dynamics, the Institute of Atmospheric Physics, the Chinese Academy of Sciences. We used the latest version 2.4.7 with triangular truncation at zonal wave number 42 (T42: equivalent to 2.81° longitude and 1.66° latitude) and 26 sigma mixing pressure levels from the ground to 2.19 hPa and time-integrating step of 10 minutes. In this model, the radiation scheme is adopted from the UK Meteorological Office (Edwards and Slingo, 1996) but with a modification from Sun and Rikus (1999a, b). The time step of the radiation scheme is 1 hour; thereby, the diurnal cycle of solar radiation was captured. The mass flux cumulus parameterization of Tiedtke (1989) is utilized for deep, shallow, and mid-level convection, with a modified closure assumption and the formation of organized entrainment and detrainment (Nordeng, 1994; Song, 2005). The planetary boundary layer part of the model is a higher-order closure scheme that computes the turbulent transfer of momentum, heat, moisture, and cloud water (Brinkop and Roeckner, 1995). The cloud scheme is a diagnostic method based on vertical motion and relative humidity (Liu and Wu, 1997), and the effects of gravity wave drag are also applied, which depend on wind speed, density, and static stability of the low-level flow Palmer et al. (1986).

3. Differences of atmospheric circulation and related diabatic heating

3.1 *Circulation*

Flooding in both the Huaihe and Yangtze River valleys in the mei-yu period is the result of southwesterly winds of the East Asian summer monsoon meeting cold wind. During the mei-yu season, the stable flow pattern over the middle and high latitudes of Asia is comprised by cold, dry air confronting warm, wet air. Based on Fig. 2, 4 years were selected for composite analyses of flooding in the Huaihe and Yangtze River valleys, respectively. Figure 3 shows composite geopotential height and precipitation anomalies of the Huaihe River valley (left panel), the Yangtze River valley (middle panel) and the differences between the Huaihe and Yangtze River valleys during flooding years (right panel).

First, we focused on the atmospheric circulation characteristic of middle and high latitudes during mei-yu flooding on the Huaihe River valley. A blocking high occurred over Lake Baikal at 200 hPa upper troposphere, which is often called “single blocking” in Eurasia. Cold air along the high-pressure front formed northwesterly wind that constantly moves eastward and southward, which met warm, wet air from the Japan Sea in the Huaihe River valley (Fig. 3a). Figure 3b shows the positive signal in East China at 850 hPa of geopotential height. This indicates that the location of SAWP was much farther west and north compared to climatology. The ridge line of the SAWP tilts slightly in a southwest-northeast orientation. As a result, warm, wet air from the BOB and the Pacific along the western ridge of the SAWP confronts cold air of middle and high latitudes, resulting in persistent rainfall in the Huaihe River Basin (Fig. 3a). The abnormal location of the SAWP matches well with the rainband position migration. Geopotential height anomalies at 200 hPa and 850 hPa at middle and high latitudes present an equivalent barotropic structure (Figs. 3a and b).

Unique characteristics in atmospheric circulation can be found during mei-yu flooding in the Yangtze River valley (Figs. 3d and e). Two blocking highs can be seen over the Eurasian continent centered in the western Urals and eastern Siberia, respectively. These

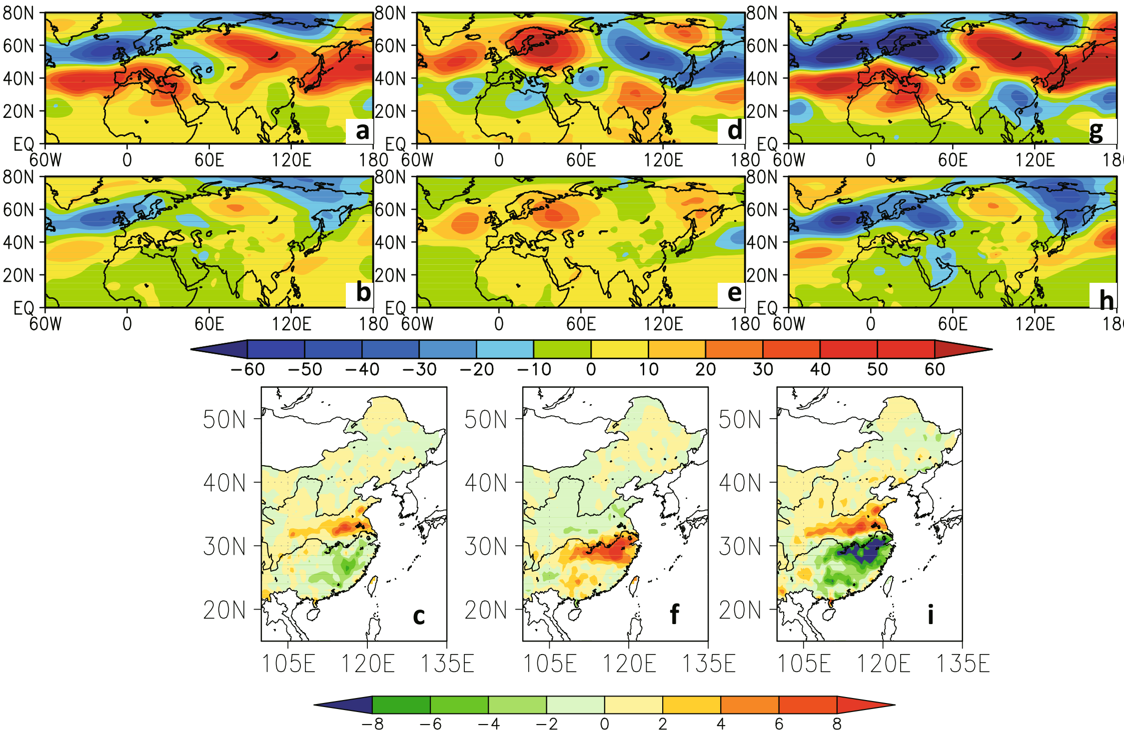

Fig. 3. Composite geopotential height anomaly at 200 hPa (top panels), at 850 hPa (middle panels) and precipitation anomaly (bottom panels) during June flooding in (a, b, c) the Huaihe River valley, (d, e, f) Yangtze River valley, and (g, h, i) the differences between them.

comprise double blocking, a pattern in the upper troposphere which is different from the single blocking associated with flooding in the Huaihe River valley (Fig. 3a). A stable low-pressure trough develops between two blockages. Cold air along the front ridge of high pressure from the northwest moves eastward and southward. The cold air is blocked by the high located over the north Okhotsk Sea and is residual in the wide trough. Figure 3d shows two wave train patterns over the Eurasian continent. One is southeastward in orientation from blocking above the Urals in the high latitudes. The other one is Pacific-Japan (PJ) wave pattern along East Asian coast. Figure 3e shows the negative signal both in central East China and the Japan Sea at 850 hPa. The ridge line of the SAWP displays zonal orientation. Equivalent barotropic structure is still obvious in middle and high latitudes during Yangtze River flooding. Furthermore, Figs. 3g, h, and i show the differences between Huaihe and Yangtze River flooding. The signal is amplified and clearer. The rainfall anomaly between the Huaihe River valley and the Yangtze River valley and its south exhibits a seesaw mode (Figs. 3c, f, and i).

We used composite analyses to demonstrate that the main differences in atmospheric circulation between flooding in the Huaihe and Yangtze River valleys are the location and intensity of SAWP and blockages at middle and high latitudes over the Eurasian continent. To confirm the relationship of the upper tropospheric circulation over the Eurasian continent and Northwest Pacific with precipitation pattern of China, the SVD method was applied to analyze coupled patterns of geopotential height at 200 hPa and June precipitation over China stations.

Figure 4 shows the spatial and temporal structure of the first two coupled modes determined from geopotential height over Eurasia and the northwest Pacific (0°–80°N, 0°–180°E) and precipitation data from 743 stations in China. The first mode accounts for 25.1% variance. Figure 4a shows that the geopotential height spatial pattern of SVD1 is similar to the composite atmospheric circulation of flooding in the Yangtze River valley. The pattern of precipitation in SVD1 shows heavy rainfall located over the Yangtze River Basin and deficient rainfall in most of North China and South China, forming a sandwich pattern. Blocking (60°N, 30°E) can be seen over the eastern Urals, wave train eastward propagation occurs with a low-high signal in the upper troposphere. The SVD2 pattern of geopotential height at 200 hPa resembles the composite result of Huaihe River flooding (Fig. 3a). Figure 4d shows blocking over Baikal,

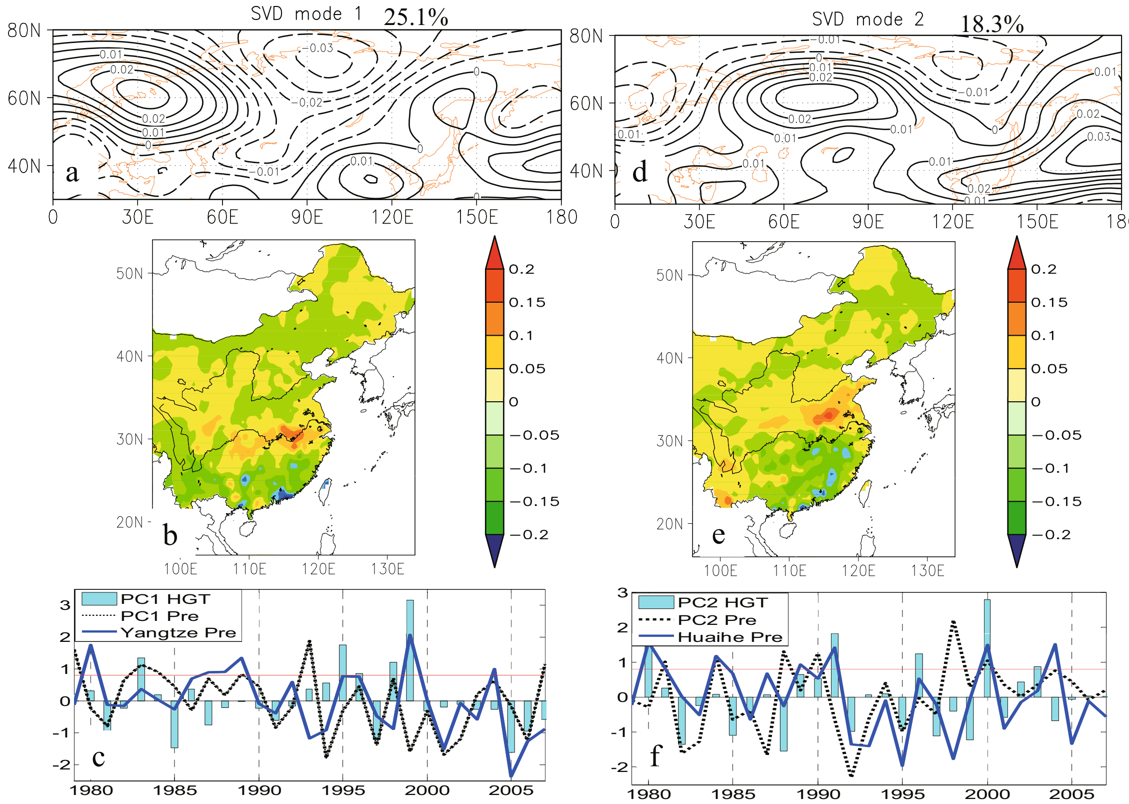

Fig. 4. The first (left panels) and second (right panels) SVD modes of June geopotential height field at 200 hPa (top, a, d) and precipitation anomaly (middle, b, e) and their standardized principal component time series (blue bar and dot line) and the Huaihe River valley and Yangtze River valley precipitation indices (blue line) (bottom, c, f).

while over the Eurasian continent the wavetrain pattern is low-high-low. Figure 4e displays the precipitation pattern, which is closely related to atmospheric circulation in Fig. 4d. The dipole mode can be seen in the rainfall signal of Huaihe River valley and northern China as opposed to the Yangtze River Basin and southern China. Figure 4e resembles Figs. 3c and i. Thus the SVD method and composite analyses collectively capture the characteristics of flooding in the Huaihe and Yangtze River valleys. Figures 4c and f show the principal components (PC) of time series and precipitation indices. The precipitation indices of the Yangtze and Huaihe River valleys are closely related to PC1 and PC2, respectively. In particular, the correlation coefficient of PC2 and Huaihe River flooding precipitation index is 0.6, far surpassing the 99% confidence level. That implies the probability of Huaihe River valley flooding in June occurring associated the atmospheric circulation at 200 hPa demonstrated by Fig. 4d that is one blocking in middle and high latitude over Eurasian continent. In order to demonstrate the relationship between precipitation and PCs time series quantitatively, Table 1 show their correlation coefficients.

Because air motion in middle and high latitudes follows quasi-geostrophic discipline, accordingly, high centers in geopotential height anomaly correspond to the anticyclone and low centers correspond to the cyclone in the wind field. But the differences of atmospheric circulation in tropic and subtropics are hardly detected in geopotential height anomalies. Composite analysis is again applied at 850 hPa wind anomaly to capture difference atmospheric circulation in low latitudes of Huaihe and Yangtze River valley flooding.

The main difference of lower tropospheric circulation is detected on meridional wind and location of anticyclone in west Pacific. Figure 5 shows composite wind anomaly and meridional wind anomaly at 850 hPa. The anticyclone anomaly over the subtropical Northwest Pacific develops both in Huaihe River flooding and in Yangtze River flooding. The anticyclone during Huaihe River flooding is located much more west and north, which influences the path of wet and warm air from the BOB and Pacific northward migration. Consequently the flooding happens in the Huaihe River valley (Fig. 3c). It is clear in Fig. 5a that winds converge nearly in 32°N much more northward compared with the climatology position. Strong northerly

Table 1. Correlated coefficient between principal components (PCs) of the (a) first SVD modes and Yangtze River precipitation, (b) second modes and Huaihe River precipitation.

(a)			
	PC1 H	PC1 Pre	Yangtze Pre
PC1 H		**0.72**	0.31
PC1 Pre			**0.50**
Yangtze Pre			
(b)			
	PC2 H	PC2 Pre	Huaihe Pre
PC2 H		**0.75**	**0.53**
PC2 Pre			**0.60**
Huaihe Pre			

Note: Bold values are above the 95% confidence level.

winds confront with southwesterly warm wet winds during flooding in the Huaihe River valley. (The cyclone anomaly near the Indian peninsula is discussed later.) The common feature in Figs. 5a and b is a strong southwest anomaly and anticyclone over both valleys. The main difference lies in meridional wind, while strong cold air converges in the Huaihe River valley (Fig. 5a) and weak zonal winds converge southwesterly in Yangtze River valley (Fig. 5b). During Yangtze River flooding June in the tropics the anticyclone over West Pacific shifts eastward and the flow becomes divergent at 850 hPa.

Although the variation of flooding areas from the center of the Huaihe River valley to the center of the Yangtze River valley is less than 5° in meridional dimension, the differences of atmospheric circulation are significant. The pattern of atmospheric circulation is not simply southward or northward migration in accordance with rainband location. What is the main factor determining the location of the rainband and its associated atmospheric circulation during early mei-yu?

3.2 *Diabatic heating*

The atmospheric motion can be viewed as a heat engine driven by diabatic heating. Atmospheric adjustment occurs in various types of energy transformation through diabatic heating. Many studies have concluded that the variation of diabatic heating in the tropics during summer monsoon is mainly caused by latent heating released from precipitation. Hoskins and Kaloly (1981) proposed the theory of quasi-steady planetary wave propagation, in which the spherical atmosphere is forced by thermal heating and large-scale mountains, which explains the mechanism of teleconnection. Theoretical investigations of stationary waves usually depend on a linearization of a zonal-mean westerly flow. Such linearization is questionable for the subtropics in the whole boreal hemisphere. In reality, during June mean state is different from that of July and multiple types of heating and/or cooling coexist. Therefore, it is worthwhile to consider how the latent heating in the tropics influences atmospheric circulation in individual months during boreal summer.

The quasi-barotropic structures in mid-high latitudes (Fig. 3) imply that the diabatic heating in the tropics may be important to determine the distinct atmospheric circulation resulting rainband location in Huaihe River valley or in the Yangtze River valley in June. Figure 6 shows the correlation of the precipitation series for the Huaihe River valley (Fig. 6a) and the Yangtze River valley (Fig. 6b), respectively with the global grid precipitation data. The precipitation of the Indian peninsula is positively correlated with the Huaihe River valley, as Fig. 6a shows. The precip-

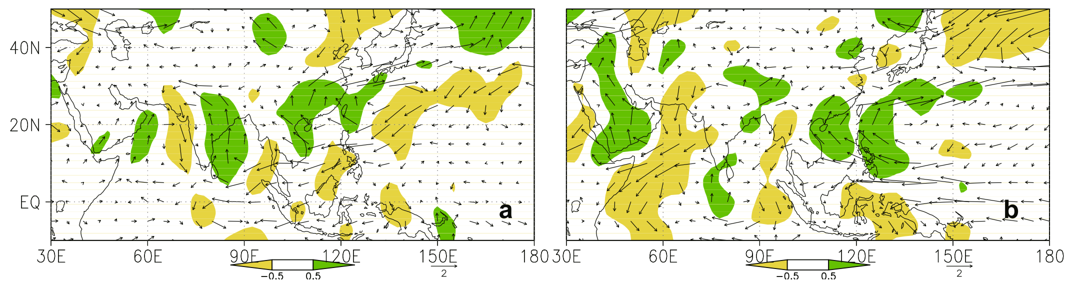

Fig. 5. Composite wind (vector) and meridional wind (shading) anomaly at 850 hPa during June flooding in (a) the Huaihe River valley, and (b) the Yangtze River valley. Units: m s^{-1}.

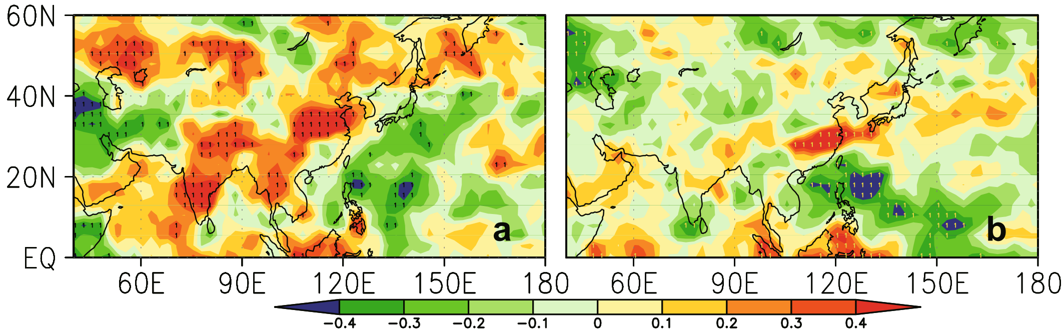

Fig. 6. Correlation coefficient of global precipitation with river valley precipitation index during June. (a) Huaihe River valley; (b) Yangtze River valley.

itation across the Tibetan Plateau and the Indo-China Peninsula are also positively correlated. Therefore, the probability for concurrence of heavy rainfall between the Huaihe River valley and the Indian peninsula is high. On the other hand, Fig. 6b shows that the rainfall over the Yangtze River valley is negatively correlated with the rainfall over the Philippine Islands and the northwestern Pacific. The diabatic heating anomaly in the tropics is mainly due to the latent heating released by precipitation. Composite outgoing long-wave radiation (OLR) (not shown) confirms that convection from the Arabian-Indian subcontinent is significantly positively related to rainfall the Huaihe River valley during Huaihe flooding, and the convection of west Pacific is negatively related to rainfall over the Yangtze River valley.

Therefore, we propose that the key areas affecting the regional rainfall in East China during June are the Indian subcontinent and the tropical West Pacific. The studies of Ding and Wang (2005, 2007) revealed that the wave train excited by diabatic heating over the Indian peninsula during summer monsoon has an important role in atmospheric circulation over the Eurasian continent at middle and high latitudes. Ding and Liu (2008) showed that, in the period of the Asian monsoon onset, a teleconnection is set up from the northwestern India via the BOB to the Yangtze River valley and southern Japan, whereas the summer rainfall in northern China is positively correlated with the Indian Summer Monsoon. Many studies have already noted the close relationship between thermal heating in the tropical West Pacific and atmospheric circulation in East Asia (Nitta, 1987; Huang and Sun, 1992). Previous studies have examined the important role of the convection in the tropical West Pacific; it influences the intensity and the variation of SAWP (Lu, 2001; Lu and Dong, 2001). Notably, these studies focused on precipitation over the whole summer. However, mean atmospheric states differ from June to August, making it necessary to focus on individual months to determine the main thermal forcing during mei-yu. Therefore, we revisited tropical heating in regulation of atmospheric circulation influencing the rain band occurring in the Huaihe River valley or the Yangtze River valley in June.

We used the mean of column integrated latent heating over the area (5°–25°N, 60°–80°E) to represent convection of the Arabian Sea and the Indian subcontinent based on Fig. 6. The correlation of geopotential height anomaly at 200 hPa with the heating across the Indian subcontinent during June is shown in Fig. 7a. Clearly, the wavetrain pattern can be seen in middle and high latitudes over Eurasia. Across the northern side of the heat source over the Indian subcontinent, the correlation coefficient is positive, indicat-

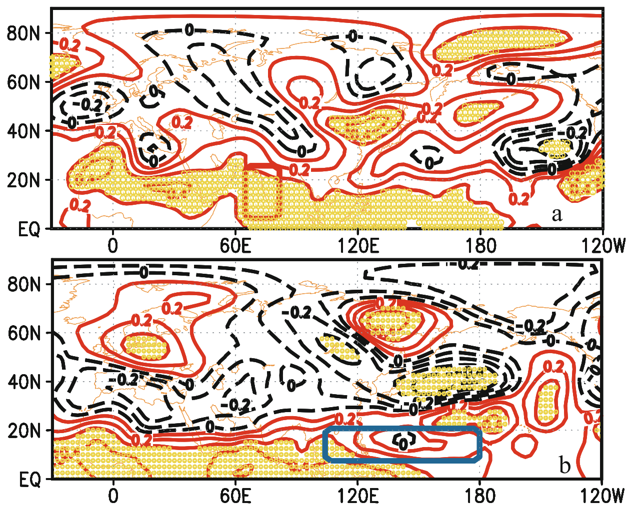

Fig. 7. Correlation of latent heating in (a, red rectangular domain) tropical Indian peninsula and (b, blue rectangular domain) tropical west Pacific with geopotential height at 200 hPa. The dotted denotes passing 90% confidence level. Compared with Fig. 3d, the pattern in Fig. 7b has the opposite signal of the correlation coefficient.

ing that heating over the Arabian-Indian subcontinent generates negative vorticity (Liu et al., 2001a). The correlation coefficient is negative over the Caspian Sea and eastern Siberia, and it is positive over Lake Baikal (Fig. 7a). The pattern is similar to that of the composite analysis of Huaihe River flooding (Fig. 3a), although the position of the blocking high deviates somewhat. From the correlation coefficient map, we can infer that when the latent heating over the Arabian-Indian peninsula is weaker the wave train signal is opposite to that shown in Fig. 7a. In this situation, there would be two ridges and one trough pattern in Eurasia similar to the upper troposphere pattern during flooding in the Yangtze River valley (Fig. 3d). Although there are slight differences between composite analyses and correlation coefficients, together they prove that the latent heating over the Indian subcontinent released by rainfall has an important role in determining precipitation in the Huaihe River and Yangtze River valleys.

The convection over the tropical West Pacific during June impacts the upper tropospheric circulation in East Asia and the Northwest Pacific. Figure 7b shows geopotential height at 200 hPa correlating with the latent heating index the tropical West Pacific (8°–20°N, 105°–180°E), a key area. The pattern is apparent, with positive correlation in Western Europe and negative correlation over Lake Baikal and eastern Siberia from west to east in Eurasia, quite similar to the pattern in Fig. 3d. The convection in west tropical Pacific obviously affects summer climate in East China. Suppressed latent heating excites a meridional teleconnection in East Asia and the West Pacific with a divergent flow anomaly over the Yangtze River valley. However, compared with composite figures, the main difference between Western Europe and Central Asia implies that other forces may exert certain regulation effects in the upper troposphere. Based upon our analysis, the upper troposphere over the Eurasian continent is largely influenced through teleconnection by convection of Arabian-Indian subcontinent during June. As for East Asia and the West Pacific, the role of latent heating released by rainfall in the tropical West Pacific may be more important. Therefore, the location of rain band during June is influenced by convection over both the Arabian-Indian subcontinent and the tropical West Pacific. Lu and Lin (2009) demonstrated that the role of subtropical precipitation anomaly itself in maintaining meridional teleconnection over the western North Pacific and East Asia should not be underestimated. The differences between Fig. 3 and Fig. 7 may reflect the impact of the latent heating released by heavy precipitation over the Huaihe or Yangtze River valleys.

4. Sensitivity experiments

In this section we report our AGCM sensitive experiments performed to test the hypothesis that abnormal latent heating in the Indian subcontinent and tropical West Pacific influence the location of the rain band in East China during the mei-yu front in June. The atmospheric response induced by the imposed latent heating anomalies during June over the Arabian-Indian subcontinent and the West Pacific were investigated separately. The control run experiment was integrated for 10 years, forced by sea surface temperature with seasonal cycles. To eliminate the model adjustment process, the mean of the latter 7 years from the 10-year integration derived from control run and sensitive experiment was adopted for analysis. The heating anomaly experiment performed over the Indian subcontinent (5°–27°N, 60°–80°E) centered at (16°N, 70°E) is referred to as EXP1. The analysis of atmospheric response is the result of EXP1 minus the control run. In the second sensitive experiment (EXP2) a latent heating anomaly was imposed over the West Pacific (4°–14°N, 110°–180°E) centered at (10°N, 150°E). The horizontal structure of heating is cosine squared (Figs. 8a, c and Figs. 9a, c in contour), and its vertical profile maximum was set at 400 hPa due to deep convection in the tropics (cf. Liu et al., 2001a, b).

The anomaly strength setting in the two sensitivity experiments was based on that in the composite from observation data. According to composite analyses using GPCP data (not shown) during Huaihe River flooding years, the precipitation anomaly over the Arabian-Indian subcontinent was ∼33% of its climatologic mean precipitation. The maximum condensation rate over the Arabian-Indian subcontinent in the control run was ∼20 K d^{-1} at 500 hPa. Therefore, the maximum anomaly of latent heating imposed in EXP1 was 7 K d^{-1}. The maximum condensation rate of West Pacific in EXP2 was set at 5 K d^{-1}, 50% of the control run (9 K d^{-1}). According to our data analyses in section 3, Yangtze River valley flooding is related to cooling in the tropical West Pacific. So we analyzed EXP2 results based on the output of the control run minus the West Pacific experiment.

4.1 *Indian subcontinent heat source*

Figure 8 shows the responses of circulation induced by the heating anomaly. The wind response demonstrates that there was obvious northerly wind in the upper troposphere (Fig. 8a) and southerly wind at the lower level (Fig. 8c) in the central and southern regions of the heating, following the Sverdrup balance (Liu et al., 2001a). An anticyclone developed northwest of the

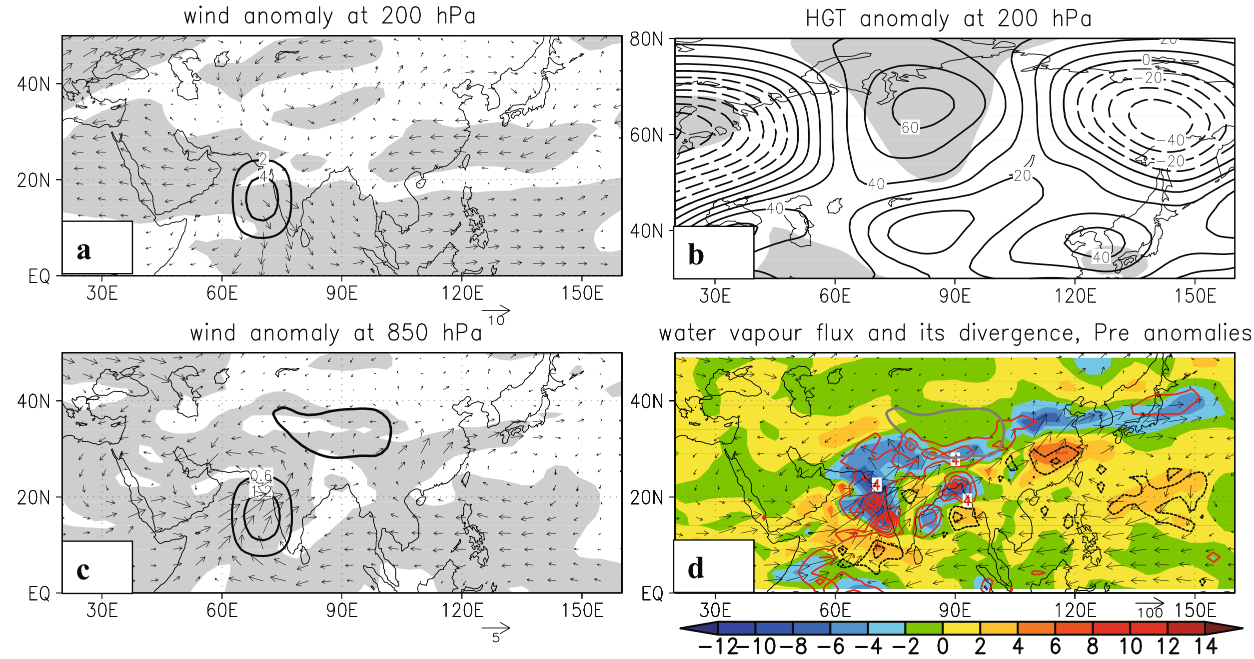

Fig. 8. Response to Indian heating anomaly in EXP1. (a) wind anomaly (vector) and heating rate (contours) at 200 hPa; (b) geopotential height anomaly at 200 hPa; (c) wind anomaly (vector) and heating rate (contours) at 850 hPa; (d) water vapor transport (vector) and its divergence (shading) and precipitation (contour) anomaly. The shading denotes passing the 90% confidence level in Figs. 8a–c. Contour interval is 2 K d^{-1} in Fig. 8a, 0.6 K d^{-1} in Fig. 8c.

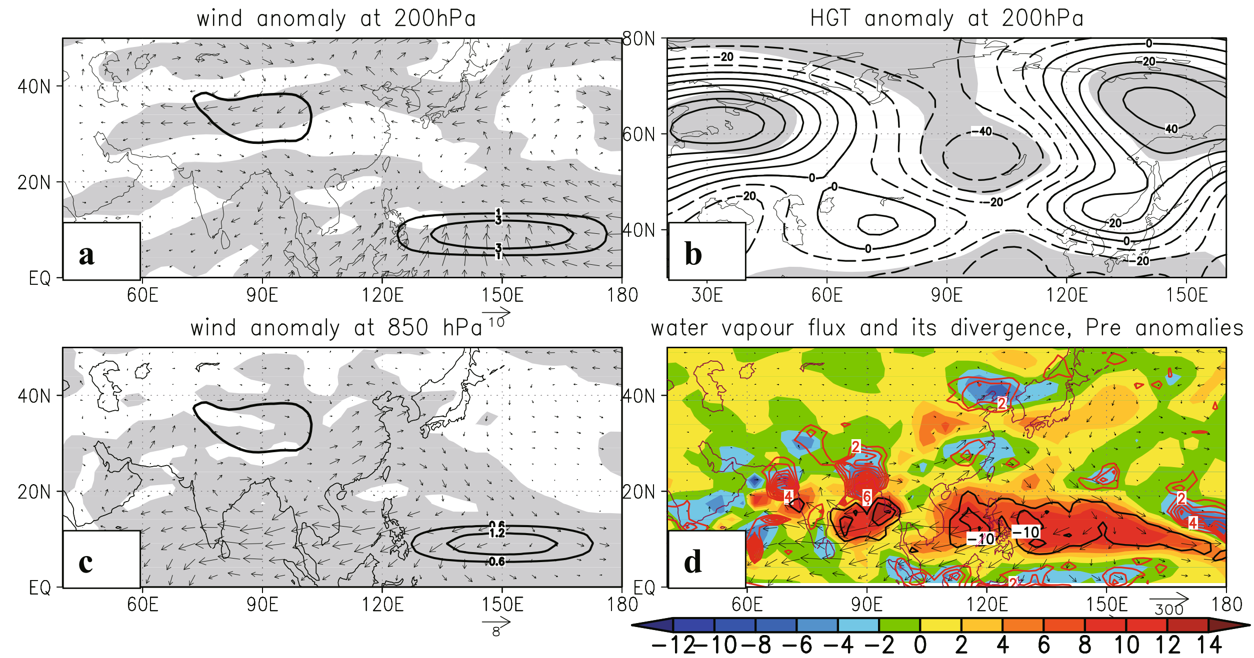

Fig. 9. Same as Fig. 8 but for cooling over tropical West Pacific in EXP2.

heating in the upper troposphere. Figure 8b shows a noticeable wave train pattern over the Eurasian continent that resembles the upper troposphere pattern related to Huaihe River valley flooding. Comparing Fig. 8a with Fig. 8c, the baroclinic structure is dominant in tropic. At 850 hPa (Fig. 8c) there is a cyclone anomaly northwest of the heating and an anticyclone over the northwest Pacific, with an anomalous southwesterly wind. Easterly wind prevails east of the heating by means of Kelvin wave propagation and west of the heating the westerly wind is obviously induced by a Rossby wave in the lower troposphere. This response can be explained by the theoretic study by Gill (1980), which adopted a simple linear model to study the response of heating symmetry on the tropics. Figure 8d shows the response of the precipitation and column-integrated water vapor divergence. The strengthened condensation forces southerly wind in the center of the Indian peninsula and south of the TP. Because of the dynamical block induced by the TP, the southerly wind changes direction, becoming easterly and southwesterly. The southwesterly wind meets southerly wind from the West Pacific, resulting in abundant precipitation over the Huaihe River valley. The convergence of anomalous water vapor in a long and narrow belt occurs along the southern flank of the TP, orienting toward the Huaihe River valley and the Japan Sea in accordance with a positive precipitation anomaly. During the mei-yu front, the water vapor over the Huaihe River valley mainly originates from the Indian peninsula and the Pacific Ocean. The results of EXP1 validate the hypothesis that latent heating released by convection over the Indian peninsula has an important role in flooding on the Huaihe River valley during mei-yu in June.

4.2 *West Tropical Pacific heat sink*

The aforementioned analysis indicates that the precipitation over the Yangtze River valley during June is closely negatively correlated with the convection in neighborhood of the Philippine Islands. The response to a heating sink from EXP2 is presented in Fig. 9. The response is similar to the composite analysis for flooding years in the Yangtze River valley. In upper troposphere (Figs. 9a and 9b), the southerly winds along the center of the cooling as well as a cyclone over south of China can be identified. The typical quasi-baroclinic structure is mainly in the subtropical region of China, complying with thermal adaption proposed by Liu et al. (2001b). Rossby wave propagations are dominant in middle and high latitudes, with two ridges over the Ural Mountains and eastern Siberia and one trough over Lake Baikal identical to the composite pattern of Yangtze River valley during flooding. In the lower troposphere (Fig. 9c), the anticyclone anomaly which is dominant in southeast China is located northwest of the cooling. The easterly anomaly prevails to the west of the cooling, even extending to the Indian peninsula at 850 hPa. Water vapor converges in South China, causing heavy precipitation, especially in the Yangtze River valley. The dipole mode is comprised of negative precipitation over the West Pacific and positive precipitation the Yangtze River valley. Precipitation is deficient in the Huaihe River valley and is abundant in north China. On the whole, the rainfall pattern looks like "sandwich" in East China induced by the sensitive experiment imposing heating in the West Pacific.

5. Discussion and conclusions

The differences of atmospheric circulation between the flooding in the Huaihe River valley and the Yangtze River valley during the mei-yu front in June have been investigated using observation and reanalysis data. The role of latent heating in key tropical areas, including the Indian peninsula and the tropical West Pacific, in regulating general atmospheric circulation anomaly over subtropical and mid-high latitudes favoring June flooding in the Huaihe River valley or Yangtze River valley has been studied with data analysis and AGCM experiment. At last the results of sensitive experiments confirm the hypothesis we proposed. Our main conclusions are the following:

(1) In the upper troposphere, the common feature is the quasi-barotropic structure in mid-high latitudes associated with Rossby wave propagation. The Rossby wavelength is longer during June flooding in the Huaihe River valley than in the Yangtze River valley. In mid-high latitudes, the signal of the wave phase is characterized with single blocking located over Lake Baikal over the Eurasian continent during flooding in the Huaihe River valley, while two ridges and one trough characterized by one blockage over the Ural Mountains and another over eastern Siberia during flooding in the Yangtze River valley.

(2) An anticyclone in low troposphere locates at Northwest Pacific penetrating in southeastern China in both the Huaihe and Yangtze River valleys during June flooding. The difference is the location of the anticyclone, which is farther north during Huaihe River flooding. Although convergence in the lower troposphere with precipitation occurs in both valleys, southwesterly wind converges with strong northerly wind during Huaihe River flooding, and southwestly wind converges with weak easterly wind during Yangtze River flooding.

(3) Convection in distinct key areas has different and important roles in heavy rainfall occurring in the

Huaihe River valley and the Yangtze River valley. Numerical sensitivity experiments verify that the latent heating imposed over the Indian peninsula could induce heavy rainfall in the Huaihe River valley and the region to its north. In low troposphere the heating induces local southerly and a Matsuno-Gill pattern response. The southerly persists to the southern flank of the TP and transports large amounts of water vapor to the south of the TP and the Huaihe River valley; enhanced precipitation even stretches to the Japan Sea. The anticyclone over Northwest Pacific (Fig. 8c) in lower troposphere and Rossby waves in the upper troposphere are similar to the pattern during Huaihe River flooding. As for heavy precipitation in the Yangtze River valley, the cooling over the tropical Western Pacific generates a PJ pattern along the East Asian coast. An anticyclone anomaly locates in northwest Pacific in the lower troposphere. A seesaw mode in precipitation occurs between the tropical West Pacific and South China, including the Yangtze River valley. These results may include important implications for the predictability of the East Asian summer climate that convection of different key areas exerts distinct influences on the flooding in the Huaihe River and Yangtze River valleys during early mei-yu.

Mei-yu flooding also frequently occurs in July. The mean flow and the associated baroclinicity in July are quite different from June. Further work will be devoted to the differences in heavy precipitation in July between the Huaihe River valley and Yangtze River valley.

Acknowledgements. We wish to thank Profs. WU Guoxiong and JI Liren for their thoughtful and constructive comments. We also appreciate the two anonymous reviewers whose comments and suggestions helped to improve the paper greatly. This work was jointly supported by the National Natural Science Foundation of China (Grant No. 40925015), and the National Program on Key Basic Research Project (Grant Nos. 2010CB950403 and 2012CB417203).

REFERENCES

Bao, Q., Y. M. Liu, T. J. Zhou, Z. Z. Wang, G. X. Wu, and P. F. Wang, 2006: The sensitivity of the spectral atmospheric general circulation model of LASG/IAP to the land process. *Chinese J. Atmos. Sci.*, **30**, 1077–1090. (in Chinese)

Bretherton, C. S., C. Smith, and J. M. Wallace, 1992: An inter-comparison of methods for finding coupled patterns in climate data. *J. Climate*, **5**, 541–560.

Brinkop, S., and E. Roeckner, 1995: Sensitivity of a general-circulation model to parameterizations of cloud-turbulence interactions in the atmospheric boundary-layer. *Tellus*(A), **47**, 197–220.

Chang, C.-P, Y. Chang, and T. Li, 2000: Interannual and inter-decadal variations of the East Asian summer monsoon and tropical Pacific SSTs. Part I: Role of the subtropical ridge. *J. Climate*, **13**, 4310–4325.

Ding, Q. H., and B. Wang, 2005: Circumglobal teleconnection in the northern hemisphere summer. *J. Climate*, **18**, 3483–3505.

Ding, Q. H., and B. Wang, 2007: Intraseasonal teleconnection between the Eurasian wavetrain and Indian summer monsoon. *J. Climate*, **20**, 3751–3767.

Ding, Y. H., and Y. Y. Liu, 2008: A study of the teleconnection in the Asian Pacific monsoon region. *Acta Meteorologica Sinica*, **66**, 670–682. (in Chinese)

Ding, Y. H., Z. Wang, and Y. Sun, 2007: Inter-decadal variation of the summer precipitation in East China and its association with decreasing Asian summer monsoon. Part I: Observed evidences. *Int. J. Climatol.*, **28**, 1139–1161.

Edwards, J. M., and A. Slingo, 1996: A studies with a flexible new radiation code. I: Choosing a configuration for a large-scale model. *Quart. J. Roy. Meteor. Soc.*, **122**, 689–720.

Gill, A. E., 1980: Some simple solutions for heat induced tropical circulation. *Quart. J. Roy. Meteor. Soc.*, **106**, 447–462.

Guo, L., and Y. M. Liu, 2008: The effects of diabatic heating on asymmetric instability and the Asian extreme climate events. *Meteor. Atmos. Phys.*, **100**, 195–206.

Hagos, S. M., and C. D. Zhang, 2010: Diabatic heating, divergent circulation and moisture transport in the African monsoon system. *Quart. J. Roy. Meteor. Soc.*, **136**, 411–425.

Hoskins, B. J., and D. J. Kaloly, 1981: The linear response of a spherical atmosphere to thermal and orographic forcing. *J. Atmos. Sci.*, **38**, 1179–1196.

Hoskins, B. J., and M. J. Rodwell, 1995: A model of the Asian summer monsoon. Part I: The global scale. *J. Atmos. Sci.*, **52**, 1329–1340.

Huang, R. H., and F. Sun, 1992: Impacts of the tropical western Pacific on the East Asian summer monsoon. *J. Meteor. Soc. Japan*, **70**, 243–256.

Huang, R. H., Y. H. Xu, and L. T. Zhu, 1999: Interdecadal variation and dry trend of summer precipitation in China. *Plateau Meteorology*, **18**, 465–476. (in Chinese)

Huang, R. H., L. T. Zhou, and W. Chen, 2003: The progresses of recent studies on the variabilities of the East Asian monsoon and their causes. *Adv. Atmos. Sci.*, **20**, 55–69.

Lau, K.-M., K.-M. Kim, and S. Yang, 2000: Dynamical and boundary forcing characteristics of regional components of the Asian summer monsoon. *J. Climate*, **13**, 2461–2482.

Liu, H., and G. X. Wu, 1997: Impacts of land surface on climate of July and onset of summer monsoon: A study with an AGCM plus SSiB. *Adv. Atmos. Sci.*, **14**, 289–308.

Liu, Y. M., H. Liu, P. Liu, and G. X. Wu, 1999: The effect of spatially non-uniform heating on the formation and variation of subtropical high. Part II: Land surface sensible heating and east Pacific-north America subtropical high. *Acta Meteorologica Sinica*, **57**, 385–396. (in Chinese)

Liu, Y. M., G. X. Wu, H. Liu, and P. Liu, 2001a: Dynamical effects of condensation heating on the subtropical anticyclones in the Eastern Hemisphere. *Climate Dyn.*, **17**, 327–338.

Liu, Y. M., G. X. Wu, R. C. Yu, and X. Liu, 2001b: Thermal adaptation, overshooting, dispersion and subtropical anticyclone, II. Horizontal inhomogeneous heating and energy dispersion. *Chinese J. Atmos. Sci.*, **24**, 317–328. (in Chinese)

Liu, Y. M., G. X. Wu, and R.C. Ren, 2004: Relationship between the Subtropical Anticyclone and Diabatic Heating. *J. Climate*, **17**, 682–698.

Lu, R., 2001: Interannual variability of the summertime North Pacific subtropical high and its relation to atmospheric convection over the Warm Pool. *J. Meteor. Soc. Japan*, **79**, 771–783.

Lu, R., and Z. D. Lin, 2009: Role of subtropical precipitation anomalies in maintaining the summertime meridional teleconnection over the western north Pacific and East Asia. *J. Climate*, **22**, 2058–2072.

Lu, R., and B. W. Dong, 2001: Westward extension of North Pacific subtropical high in summer. *J. Meteor. Soc. Jap*an, **79**, 1229–1241.

Ma, Y., W. Chen, and L. Wang, 2011: A comparative study of the interannual variation of summer rainfall anomalies between the Huaihe Mei-yu season and the Jiangnan Mei-yu season and their climate background. *Acta Meteorologica Sinica*, **69**, 334–343. (in Chinese)

Nitta, T., 1987: Convective activities in the tropical western Pacific and their impacts on the Northern Hemisphere summer circulation. *J. Meteor. Soc. Japan*, **65**, 373–390.

Nordeng, T. E., 1994: Extended versions of the convective parameterization scheme at ECMWF and their impact on the mean and transient activity of the model in the tropics. ECMWF Technical Memo. No. 206, Reading, England, 41pp.

Palmer, T. N., G. J. Shutts, and R. Swinbank, 1986: Alleviation of a systematic westerly bias in general circulation and numerical weather prediction models through an orographic gravity wave drag parameterization. *Quart. J. Roy. Meteor. Soc.*, **112**, 1001–1039.

Rodwell, M. J., and B. J. Hoskins, 2001: Subtropical anticyclones and summer monsoons. *J. Climate*, **14**, 3192–3211.

Smagorinsky, J., 1953: The dynamical influence of large scale heat sources and sinks on the quasi-stationary mean motions of the atmosphere. *Quart. J. Roy. Meteor. Soc.*, **79**, 342–366.

Song, X. L., 2005: The evaluation analysis of two kinds of mass flux cumulus parameterizations in climate simulation. Ph. D. dissertation, Institute of Atmospheric Physics, Chinese Academy of Sciences, 119–145. (in Chinese)

Sun, Z., and L. Rikus, 1999a: Improved application of ESFT to inhomogeneous atmosphere. *J. Geophys. Res.*, **104**, 6291–6303.

Sun, Z., and L. Rikus, 1999b: Parameterization of effective radius of cirrus clouds and its verification against observations. *Quart. J. Roy. Meteor. Soc.*, **125**, 3037–3056.

Tao, S. Y., and L. X. Chen, 1987: A review of recent research of the East Asian summer monsoon in China. *Monsoon Meteorology*, C.-P. Chang and T. N. Krishnamurti, Eds., Oxford University Press, 60–92.

Tao, S. Y., and J. Wei, 2006: The westward, northward advance of the Subtropical High over the west Pacific in summer. *Quarterly Journal of Applied Meteorology*, **17**, 513–525. (in Chinese)

Tiedtke, M., 1989: A comprehensive mass flux scheme for cumulus parameterization in large-scale models. *Mon. Wea. Rev.*, **117**, 1779–1800.

Ting, M. F., and H. Wang, 1997: Summertime US precipitation variability and its relation to Pacific sea surface temperature. *J. Climate*, **10**, 1853–1873.

Wang, B., J. Liu, J. Yang, T. J. Zhou, and Z. W. Wu, 2009: Distinct principal modes of early and late summer rainfall anomalies in East Asia. *J. Climate*, **22**, 3864–3875.

Wang, H., and Q. Q Wang, 2002: Relationship between summer precipitation anomalies in the Huaihe basin and SSTA over the North Pacific. *Journal of Nanjing Institute of Meteorology*, **25**, 45–54. (in Chinese)

Wang, Z. Z., G. X. Wu, T. W. Wu, and R. C. Yu, 2004: Simulation of the seasonal variations of Asian monsoon with the climate model R42L9/LASG. *Adv. Atmos. Sci.*, **21**, 879–889.

Wei, F. Y., and T. Zhang, 2009: Oscillation characteristics of summer precipitation in the Huaihe River valley and relevant climate background. *Science in China (D)*, **39**, 1360–1374. (in Chinese)

Wu, G. X., and Y. M. Liu, 2000: Thermal adaptation, overshooting, dispersion and subtropical anticyclone, I. Thermal adaptation and overshooting. *Chinese J. Atmos. Sci.*, **24**, 433–446. (in Chinese)

Wu, G. X., and Y. M. Liu, 2003: Summertime quadruplet heating pattern in the subtropics and the associated atmospheric circulation. *Geophys. Res. Lett.*, **30**, 1201–1204.

Wu, G. X., H. Liu, Y. C. Zhao, and W. P. Li, 1996: A nine-layer atmospheric general circulation model and its performance. *Adv. Atmos. Sci.*, **13**, 1–18.

Wu, G. X., Y. M. Liu, and P. Liu, 1999: Spatially inhomogeneous diabatic heating and its impacts on the formation and variation of subtropical anticyclone, I. Scale analysis. *Acta Meteorologica Sinica*, **57**, 257–263. (in Chinese)

Wu, G. X., and Y. M. Liu, J. J. Yu, X. Y. Zhu, and R. C. Ren, 2008: Recent progresses in studies of the temporal-spatial variations of the East Asian monsoon system and their impacts on climate anomalies in China. *Chinese J. Atmos. Sci.*, **32**, 720–740. (in Chinese)

Wu, T. W., Z. Z. Wang, Y. M. Liu, R. C. Yu, and G. X. Wu, 2004: An evaluation of the effects of cloud parameterization in the R42L9 GCM. *Adv. Atmos. Sci.*, **21**, 153–162.

Xu, H. M., J. H. He, and M. Dong, 2001: Numerical study of the effect of Indian Peninsula on south Asian summer monsoon process. *Journal of Tropical Meteorology*, **17**, 117–124. (in Chinese)

Xuan, S. L., Q. Y. Zhang, and S. Q. Sun, 2011: Relationship between the monthly variation of the East Asia westerly jet and the Huaihe River valley rainfall anomaly in summer. *Climatic and Environmental Research*, **16**, 231–242. (in Chinese)

Yao, X. P., G. X. Wu, Y. M. Liu, and H. Z. Liu, 2007: Case study on the impact of the vortex in the easterlies over the tropical upper troposphere on the subtropical anticyclone over western Pacific ocean. *Acta Meteorologica Sinica*, **65**, 198–207. (in Chinese)

Zhang, Q. Y., and S. Y. Tao, 1998: Influence of Asian mid-high latitude circulation on East Asian summer rainfall. *Acta Meteorologica Sinica*, **56**, 199–211. (in Chinese)

Zhao, B. K., X. P. Yao., and G. X. Wu, 2005: The structure and activity characteristics of the western Pacific subtropical anticyclone and its dynamical mechanism during the Meiyu period over the Huaihe River basin in 2003. *Chinese J. Atmos. Sci.*, **29**, 771–779. (in Chinese)

Zhou, L. T., and R. H, Huang, 2003: Research on the characteristics of interdecadal variability of summer climate in China and its possible cause. *Climatic and Environmental Research*, **8**, 274–290. (in Chinese)